BBA - Biomembranes 1860 (2018) 1205–1215

Contents lists available at ScienceDirect

BBA - Biomembranes

journal homepage: www.elsevier.com/locate/bbamem

Effect of ubiquinone-10 on the stability of biomimetic membranes of relevance for the inner mitochondrial membrane

Emma K. Eriksson, Víctor Agmo Hernández, Katarina Edwards*

Department of Chemistry-BMC, Uppsala University, Box 579, SE-75123 Uppsala, Sweden

ARTICLE INFO

Keywords:
Coenzyme Q10
Biomimetic membranes
Liposomes
Membrane stability
Solanesol

ABSTRACT

Ubiquinone-10 (Q10) plays a pivotal role as electron-carrier in the mitochondrial respiratory chain, and is also well known for its powerful antioxidant properties. Recent findings suggest moreover that Q10 could have an important membrane stabilizing function. In line with this, we showed in a previous study that Q10 decreases the permeability to carboxyfluorescein (CF) and increases the mechanical strength of 1-palmitoyl-2-oleyl-sn-glycero-phosphocholine (POPC) membranes. In the current study we report on the effects exerted by Q10 in membranes having a more complex lipid composition designed to mimic that of the inner mitochondrial membrane (IMM). Results from DPH fluorescence anisotropy and permeability measurements, as well as investigations probing the interaction of liposomes with silica surfaces, corroborate a membrane stabilizing effect of Q10 also in the IMM-mimicking membranes. Comparative investigations examining the effect of Q10 and the polyisoprenoid alcohol solanesol on the IMM model and on membranes composed of individual IMM components suggest, moreover, that Q10 improves the membrane barrier properties via different mechanisms depending on the lipid composition of the membrane. Thus, whereas Q10's inhibitory effect on CF release from pure POPC membranes appears to be directly and solely related to Q10's lipid ordering and condensing effect, a mechanism linked to Q10's ability to amplify intrinsic curvature elastic stress dominates in case of membranes containing high proportions of palmitoyl-2-oleoyl-sn-glycero-3-phosphoethanolamine (POPE).

1. Introduction

Ubiquinones are lipid soluble molecules present in the lipid membranes of most eukaryotic cells and gram-negative bacteria [1,2]. They were first found in beef heart mitochondria while exploring the components of the respiratory chain [3]. The ubiquinones consist of a long isoprenoid chain attached to a substituted quinone headgroup (Fig. 1a). In humans, the most common ubiquinone contains a chain built from 10 isoprenoid units and the molecule is therefore referred to as ubiquinone-10 (Q10) or Coenzyme Q10. Q10 is well known to mediate electron and proton transport through the mitochondrial membrane for energy conversion purposes [4,5]. In its reduced form, ubiquinol, the molecule also scavenges free radicals and thereby protects the lipids from oxidation [6,7]. Q10 has moreover been suggested to play an important role in cell growth and certain forms of apoptosis [8–10]. Altered Q10 tissue levels have been associated to several illnesses, the most widely studied being neurodegenerative and cardiovascular diseases [11–13]. Low levels have also been found in some cancer patients [13–15].

Accumulating evidence suggest that ubiquinones, beside their above-mentioned roles as electron-/proton-carriers and antioxidants, could have a stabilizing function in biological membranes. In support of this hypothesis it has been observed that bacteria increase their production of endogenous ubiquinone-8 when subjected to hyperosmotic salt stress [16,17]. Further, we have in a previous study reported on the ability of Q10 to modulate the intrinsic properties of lipid membranes [18]. More specifically, results from investigations based on palmitoyl oleoyl phosphatidylcholine (POPC) liposomes show that inclusion of ubiquinone leads to increased lipid packing order and higher membrane density, as well as decreased permeability and higher membrane mechanical stability. These findings are interesting not least given that Q10 is particularly abundant in certain biological membranes, such as the inner mitochondrial membrane (IMM), where the content of the well-known membrane stabilizer cholesterol is low. However, although

Abbreviations: CerPEG5000, *N*-palmitoyl-sphingosine-1-[succinyl(methoxy(polyethylene glycol)5000)]; CF, carboxyfluorescein; CL, cardiolipin (heart, bovine); DPH, 1,6-diphenyl-1,3,5-hexatriene; IMM, inner mitochondrial membrane; POPE, 1-palmitoyl-2-oleyl-sn-glycero-phosphoethanolamine; POPC, 1-palmitoyl-2-oleyl-sn-glycero-phosphocholine; POPS, 1-palmitoyl-2-oleoyl-sn-glycero-3-[phospho-L-serine] sodium salt; Q10, ubiquinone-10, coenzyme Q10; Soy-PI, L-α-phosphatidylinositol (soy) sodium salt; Soy-PS, L-α-phosphatidylserine (soy) sodium salt

* Corresponding author.
E-mail addresses: emma.eriksson@kemi.uu.se (E.K. Eriksson), victor.agmo@kemi.uu.se (V. Agmo Hernández), katarina.edwards@kemi.uu.se (K. Edwards).

https://doi.org/10.1016/j.bbamem.2018.02.015
Received 29 September 2017; Received in revised form 13 February 2018; Accepted 15 February 2018
Available online 19 February 2018

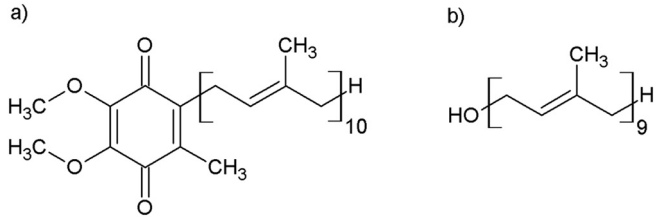

Fig. 1. Molecular structure of a) ubiquinone-10 and b) solanesol.

POPC is a biologically relevant lipid component, it needs to be realized and stressed that native biological membranes as a rule contain a complex mixture of different lipid species. It is conceivable that alterations in the lipid composition can lead to changes in lipid spontaneous curvature, membrane bending rigidity, and other micromechanical properties that affect Q10's interaction with, and impact on, the membrane. In line with this, molecular dynamics simulations indicate that ubiquinone-lipid interactions vary depending on the lipid species [19,20]. Also, the interaction between Q10 and lipid monolayers has been shown to be affected by the nature of the lipid headgroup, the acyl chain length and the degree of unsaturation [21,22]. In order to further explore and confirm the membrane stabilizing function of Q10 it is therefore important to verify that the effects observed on POPC membranes persist when the lipid composition is changed and adapted to more closely reflect that of native biological membranes.

In the present study we have investigated the effect of ubiquinone on the lipid packing and barrier properties of membranes with a lipid composition resembling that of the inner mitochondrial membrane (IMM). A relevant feature of the IMM, which typically contains Q10 in comparably large proportions (0.5–2 mol%, related to the lipid content [23,24]), is the high content (~49 mol%) of phosphoethanolamine (PE) lipids, as well as the presence of substantial proportions (~6 mol%) of cardiolipin (CL) [25]. It is plausible that the presence of these lipids could have an important influence on the Q10-membrane interactions.

In order to learn more about the specific impact of CL and PE lipids, we have, in addition to studies involving the multicomponent IMM-mimicking membranes, performed experiments based on the use of membranes composed of a single or a reduced number of lipid components. Finally, to reveal more details about the Q10-lipid interactions we have carried out comparative studies using solanesol, a molecule very similar to Q10 but lacking the quinone ring (see Fig. 1b), and hexadecane, a long fully hydrophobic molecule.

2. Materials and methods

2.1. Chemicals

Cardiolipin (CL) from bovine heart sodium salt, 1-palmitoyl-2-oleoyl-sn-glycero-3-phosphoethanolamine (POPE), soy L-α-phosphatidylinositol (Soy-PI) sodium salt, soy L-α-phosphatidylserine (soy) (Soy-PS)sodium salt, 1-palmitoyl-2-oleoyl-sn-glycero-3-[phospho-L-serine] (POPS) sodium salt and *N*-palmitoyl-sphingosine-1-[succinyl(methoxy (polyethylene glycol)5000)] (cerPEG5000) were bought from Avanti Polar Lipids (Alabaster, USA). 1-palmitoyl-2-oleyl-sn-glycero-phosphocholine (POPC) was obtained as a kind gift from Lipoid Gmbh (Ludwigshafen, Germany). Ubiquinone-10 (Q10), solanesol (from tobacco leaves), cholesterol, polyethylene glycol *tert*-octylphenyl ether (Triton X-100), 5(6)-carboxyfluorescein (CF), octaethylene glycol monododecyl ether ($C_{12}E_8$), 1,6-diphenyl-1,3,5-hexatriene (DPH), ammonium molybdate ($(NH_4)_6Mo_7O_{24}{\cdot}4H_2O$), sulfuric acid, methanol (Chromasolv® for HPLC, ≥ 99.9%), Hepes (> 99.5%), sodium dodecylsulfate (SDS), sodium chloride, sodium phosphate monobasic dihydrate, sodium phosphate dibasic dihydrate, and hexadecane (Regentplus®, 99%) were purchased from Sigma-Aldrich (Steinheim, Germany). Chloroform (pro analysis), potassium antimony tartrate hemihydrate ($K(SbO)C_4H_4O_6{\cdot}0.5H_2O$) and L(+)-ascorbic acid were products from MERCK (Darmstadt, Germany). Hexane (> 98%, mixed isomers) was a product from Acros Organics (Geel, Belgium). 99.7% spectroscopic grade ethanol was from Solveco (Rosersberg, Sweden). A phosphate buffered saline (PBS, 10 mM phosphate, 150 mM NaCl) was used for the measurements performed at a controlled pH value of 7.4. All aqueous solutions were prepared using deionized water (18.2 MΩ cm) obtained from a Milli-Q system (Millipore, Bedford, USA). Experiments were performed at 25 °C unless otherwise indicated.

2.2. Preparation of liposomes

The desired amount of lipid was either weighed or pipetted from stock solutions in chloroform. The lipids were further dissolved/diluted by adding extra chloroform. A lipid film was obtained by drying the mixture with nitrogen gas and removing the remaining traces of solvent under vacuum (Squaroid vacuum oven, Lab Instruments, IL, USA) overnight. The lipid film was thereafter suspended in the desired aqueous solution, typically PBS if nothing else is stated. The lipid suspension was afterwards subjected to 15 freeze-thaw cycles (freezing with liquid nitrogen, thawing with a water bath at 60 °C) for CL containing mixtures, to homogenize the suspension. For other compositions, the process was repeated only 5 times. The suspensions were thereafter extruded 31 times through a 100 nm pore size filter (Watman plc, Kent, UK) using a Lipofast extruder (Avestin, Ottawa, Canada). When necessary, suspensions which were difficult to extrude were pre-extruded 15 times through a 200 nm filter before the final 100 nm extrusion. Pure POPE liposomes and POPE liposomes supplemented with PEG-lipid were extruded at 37 °C while all the other compositions were extruded at room temperature.

Liposomes containing Q10 or solanesol where prepared as above. Q10 or solanesol was added to the lipid mixture from stock-solutions in 1:1 ethanol: chloroform before obtaining the dry lipid film. Hexadecane-containing liposomes were produced by adding a small volume of an ethanol solution of hexadecane to an already dried lipid film. The small amount of ethanol was evaporated with nitrogen gas and the lipid mixture was thereafter suspended in buffer. The aqueous mixture was bath sonicated (Branson 1210E-MT, Branson Ultrasonics Corporation, USA) for 1 h and 15 min to improve blending of the components before extruding 31 times with a 100 nm pore size filter.

After preparation, the suspensions were stored for 24 h in room temperature before starting the experiment. POPE liposomes were stored at 37 °C. The reason for storage was to assure the repeatability in the experiments, in agreement with a previous report showing that liposomes tend to reach an equilibrium state approximately 24 h after preparation [26]. This equilibration was done for all experiments except for the spontaneous leakage experiments in which the samples were used directly after preparation.

2.3. Cryo-TEM characterization

Cryogenic transmission electron microscopy (cryo-TEM) was used to analyse the morphology of the samples. In short, a drop of sample with a lipid concentration in the 1–10 mM range is placed onto a copper grid reinforced with a holey polymer film. This procedure is performed in a chamber with high humidity and temperature (normally 25 °C). The sample together with the grid is plunged into liquid ethane to vitrify the sample and thereafter transferred to the microscope. The sample was protected from atmospheric conditions and was kept below −160 °C during the transfer. A more detailed description of the sample preparation technique has been described earlier by Almgren et al. [27]. Analyses were performed with a Zeiss TEM Libra 120 instrument (Carl Zeiss AG, Oberkochen, Germany) operating in a zero-loss bright-field mode. The digital images were recorded under low-dose conditions with a BioVision Pro-SM Slow Scan CCD camera (Proscan elektronische systeme GmbH, Scheuring, Germany).

2.4. Determination of Q10 and solanesol content in the lipid membranes

The incorporated Q10 proportion in the prepared liposomes was estimated by independent determinations of the phosphorous and the Q10 content in the samples. Liposomes were prepared as described above, using Hepes buffered saline (HBS) instead of PBS. Determinations were done in triplicates. The phosphorous content of the samples was determined using the method described by Paraskova et al. [28]. Briefly, aliquots of the sample were calcinated at 550 °C and the obtained ashes were dissolved in 4 mL water. A volume of 1 mL of a freshly prepared mixture of seven parts of 1:3:10 K(SbO)-$C_4H_4O_6{\cdot}0.5H_2O$ (2.75 mg mL^{-1}): $(NH_4)_6Mo_7O_{24}{\cdot}4H_2O$ (4% w/v): H_2SO_4 (2.5 M) and three parts of ascorbic acid 0.1 M in water was then added. After 15 min, the absorbance at 882 nm of the obtained solution was measured with an UV–Vis spectrometer (HP 8453, Agilent Technologies, Santa Clara, CA, USA). The concentration of phosphorus was calculated with the help of a standard curve prepared from different volumes of a phosphorus standard solution (0.65 mM, Sigma Aldrich, St. Louis, MO, USA).

The Q10 content was determined with the method described by Kröger [29]. Briefly, a volume of 0.32 mL hexane was added to the aliquots. Then, 0.48 mL methanol was added and the samples were vortexed for 1 min, followed by addition of 0.32 mL acetone, vortex for 1 min and head-over-tail shaking for ~20 min. The sample was then centrifuged at 1500 × *g* for 2 min. The upper phase was then collected. The hexane extraction was repeated one more time and the collected organic fractions were pooled together. Hexane was then removed under a nitrogen flow, followed by incubation in a vacuum for ~2 h. Finally, 2.5 mL spectroscopic grade ethanol was added and the absorbance at 275 nm was determined. The concentration of Q10 in the sample was calculated from its molar extinction coefficient in ethanol (12.6 mM^{-1} cm^{-1}, [29]).

The procedure described above has proven useful also to determine the solanesol content in POPC liposomes, using a detection wavelength of 200 nm and the standard addition method instead of a defined extinction coefficient [18]. However, the protocol was not successful for the determination of solanesol content in IMM and POPE-containing membranes, as the standard addition curves were neither reproducible nor linear. In order to approximately estimate the amount of solanesol incorporated into IMM liposomes, POPC liposomes were used as reference. The amount of Q10 and of solanesol incorporated into POPC membranes when mixed at the same proportion was determined. The incorporation of solanesol relative to that of Q10 (i.e, incorporated solanesol fraction/incorporated Q10 fraction) was then calculated. The proportion of solanesol in IMM was assumed to follow the same trend, and was therefore estimated from the determined Q10 fraction.

2.5. Fluorescence anisotropy

The degree of order in the membrane was estimated through steady-state fluorescence anisotropy measurements. For this purpose, the hydrophobic fluorescent probe DPH was used. This probe aligns roughly parallel to the acyl chains segments and does on the average locate about midway between the bilayer centre and the membrane surface. Therefore, the results obtained in the experiment do not reflect the order in the centre of the membrane but report on the order in the hydrophobic region closer to the polar headgroups [30]. The probe was dissolved in methanol to produce a highly concentrated (0.91 mM) stock-solution and thereafter added to freshly prepared liposome samples with a probe:lipid ratio of 1:1000. The mixtures were kept at least 12 h in the dark before use in order to assure complete incorporation of the probe into the lipid membrane. The fluorescence intensities could thereafter be measured by use of a SPEX fluorolog 1650 0.2 m double spectrometer (SPEX industries, Edison, USA) in the right angle mode equipped with two polarization filters, polarizing the excitation and the emission beams respectively. The excitation wavelength was set to 357 nm and the emission wavelength was set to 424 nm. The sample was thermostated to 25 °C (unless otherwise indicated). The fluorescence intensity at all four possible combinations of the polarizing filters were measured. The fluorescence anisotropy $< r >$ was calculated by:

$$< r > = \frac{I_{VV} - GI_{VH}}{I_{VV} + G2I_{VH}} \quad (1)$$

where $G = I_{HV}/I_{HH}$ is an instrumental correction factor I_{XY} are the fluorescence intensities measured with the different combinations of the polarizers (X = excitation, Y = emission, H = horizontal, V = vertical) [31]. The experiments were performed at least in triplicates. The error margins reported correspond to the standard error of all repetitions.

2.6. Liposome leakage measurements

For all leakage experiments, the liposome suspensions were prepared in a self-quenching carboxyfluorescein (CF) solution (100 mM CF, 10 mM sodium phosphate, pH 7.4), isotonic with PBS. The extruded liposomes were thereafter separated from the non-encapsulated material, right before use, by using a PD-10 column (GE-Healthcare, Uppsala, Sweden) equilibrated with PBS. The fluorescence intensities were measured at 25 °C with a SPEX fluorolog 1650 0.2 m double spectrometer (SPEX industries, Edison, USA) in the right angle mode with the excitation and emission wavelengths set to 495 and 520 nm, respectively. Both spontaneous and detergent induced leakage assays were performed.

Samples for the spontaneous leakage experiments were diluted to a total lipid concentration of 12 μM after separation to ensure that the fluorescence was in the linear concentration-dependent signal range. Polystyrene cuvettes (Kartell Labware, Italy) were selected as the liposomes were observed to significantly interact with quartz and glass. The degree of leakage over time ($x_{CF_{rel}}(t)$) was calculated by:

$$x_{CF_{rel}}(t) = \frac{I(t) - I_0}{I_{tot} - I_0} \quad (2)$$

where $I(t)$ is the time-dependent fluorescence intensity, I_0 is the intensity at the starting point of the experiment and I_{tot} is the intensity at complete leakage from the liposomes, achieved by solubilizing the liposomes upon addition of 50 μL of 200 mM Triton X-100. The experiments were run over at least 5 h with a sampling interval of 5 s.

Samples for the detergent induced leakage experiments were diluted to a total lipid concentration of 24 μM after separation. The liposomal suspensions were mixed in a 1:1 ratio with $C_{12}E_8$ solutions at concentrations in the 0 to 5 mM range using a stop-flow apparatus (SFA-II Rapid Kinetics Accessory, TgK Scientific, England)). The highest detergent concentration was used to induce complete liposomal leakage and the result was used for normalization purposes. The degree of leakage over time was thereafter calculated using Eq. 2. The experiments were run for ~5 min with a sampling interval of 0.5 s.

2.7. $C_{12}E_8$ partition behaviour

The optical density (turbidity) of the liposomal samples was studied to probe the partitioning behaviour of $C_{12}E_8$ in the lipid membranes. A detailed description of theory and experiment can be found in our previous study [18]. In short, the experiments were carried out by adding 0.5–2 μL of concentrated stock-solutions of surfactant (50–200 mM $C_{12}E_8$) to a 2 mL volume of a liposome suspension with a known lipid concentration, and measuring the optical density at 300 nm after each addition. The experiments were performed at different initial total lipid concentrations in the range of 0.5–3 mM and in each case the onset of solubilisation was determined as the detergent concentration at which the turbidity started to decrease. The combined results were used to estimate the membrane/buffer partition coefficient (K):

$$K = \frac{R_{e[\mathrm{Sat}]}}{[S]_{\mathrm{Free}}(R_{e[\mathrm{Sat}]} + 1)} \quad (3)$$

where $R_{e[\mathrm{Sat}]}$ is the effective detergent/lipid ratio in the membrane at saturation and $[S]_{\mathrm{Free}}$ is the amount of surfactant that remains free in solution. The $R_{e[\mathrm{Sat}]}$-value can be extracted from the slope in a plot where the total surfactant concentration at the onset of solubilisation is plotted against the lipid concentration of the sample. It was assumed that $[S]_{\mathrm{Free}}$ at saturation was equal to the CMC for $C_{12}E_8$ (75 μM [32]).

2.8. QCM-D characterization

A Quartz Crystal Microbalance with Dissipation monitoring (QCM-D E1, Q-Sense, Gothenburg, Sweden) was used to study the adhesion and rupture of liposomes on silica surfaces. The temperature was set to 21 °C and a controlled sample flow of 150 μL min^{-1} was used. Frequency and dissipation data were collected from the fundamental sensor frequency (5 MHz), as well as the 3rd, 5th, 7th, 9th, 11th and 13th overtones. The silica QCM-D sensors were cleaned by placing them for 20 min in an UV/Ozone chamber (BioForce Nanosciences Inc., Ames, Iowa), followed by 30 min rinsing in a 2% SDS-solution. They were thereafter rinsed with Milli-Q water, dried with nitrogen and finally treated again for 20 min in the UV/ozone chamber. The sensors were directly mounted in the QCM-D instrument after cleaning and the system was equilibrated with the working solution (PBS). When a stable baseline had been obtained, a 12 μM suspension of liposomes in PBS was introduced into the system and was then left to react with the surface until the system was stabilized. As a last step, the system was rinsed with PBS to wash away any non-bound material.

3. Results and discussion

3.1. Liposomes mimicking the composition of the inner mitochondrial membrane (IMM)

To model the lipid composition of the inner mitochondrial membrane, the following lipids were selected: POPE: POPC: CL: Soy-PI: Soy-PS (49.2: 43: 6.1: 1: 0.7 mol ratio). This composition reflects the relative proportion of different headgroups present in the inner membrane of mitochondria from rat liver as reported by Hovius et al. [25]. Besides accurately reflecting the headgroup composition, the selected lipid composition gives a ratio between saturated and unsaturated fatty acid chains that is close to that found in rat liver mitochondria [33].

Cryo-TEM was used to confirm that the preparation method described in Section 2.2 resulted in the formation of liposomes. An obtained picture is shown in Fig. 2. The phase transition temperature between the gel and the liquid crystalline phase states was determined to be ~16 °C (see Fig. S1 in the supplementary material), which confirms that our model membrane is in the liquid crystalline phase at room temperature.

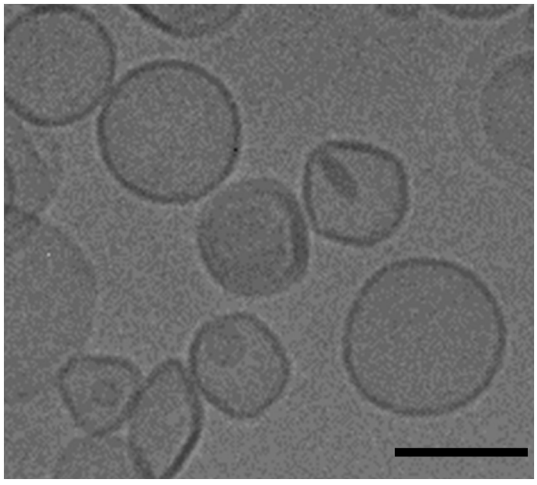

Fig. 2. Cryo-TEM image of IMM-mimicking liposomes 25 °C. The scale bar is 100 nm.

Changes in the packing order of the lipid chains in the membrane were estimated by measuring the steady-state anisotropy $< r >$ of DPH incorporated in the membrane [34–36]. In case of the IMM composition, the value of $< r >$ was determined to be 0.1235 ± 0.0011. For comparison, the corresponding value for a pure POPC membrane is 0.1026 ± 0.0019 [18]. This suggests that the lipid composition used to model the IMM results in membranes in which the hydrocarbon chains are more ordered than in membranes composed of POPC alone. Part of the reason for the higher packing order can be understood by acknowledging that the lipids in the IMM mixture collectively exhibit a negative spontaneous curvature. As a consequence of this property, which is discussed in more detail in Section 3.2.5, the hydrocarbon chains are forced to elongate and pack closely in order to assume the flat topology typical of a lipid membrane.

3.2. Effects of ubiquinone in the IMM model

The investigations presented in the following sections were performed in order to elucidate whether the stabilizing effects exerted by Q10 in POPC membranes are preserved in the IMM model.

3.2.1. Q10 and solanesol incorporation into IMM model membranes

As reported in our previous work with POPC [18], it cannot be assumed that all of the Q10 present in the original lipid mixture is incorporated into the liposome membranes. Further, above a critical concentration (proportions larger than ~6 mol% Q10 in case of the POPC system) non-bilayer structures start to appear in the preparations. We therefore characterized the IMM liposomes (prepared according to the protocol in Section 2.2 using a lipid:Q10 mixing ratio of 25:1) in terms of their lipid and Q10 content. Phosphorous analyses combined with Q10 determinations showed that only about 53% of the total Q10 added is incorporated into the liposomes, giving thus an effective Q10 content of 2.1 mol% incorporated in the lipid membrane. The results obtained with Q10 are therefore in the following sections compared with what has been determined for preparations of POPC incorporating 2 mol% Q10. Notably, as judged from cryo-TEM analyses, no non-bilayer structures were present in the IMM:Q10 preparations (see Fig. S2 in the supplementary material for a representative micrograph).

In case of IMM liposomes supplemented with solanesol, the effective lipid:solanesol ratios could, as stated in the Materials and methods section, not be determined directly. The ratios provided for IMM liposomes are therefore approximate values (denoted with the symbol ~) based on analysis of solanesol and Q10 content in pure POPC liposomes. These determinations showed that the fraction of solanesol incorporated in the POPC membrane equals roughly 70% of the fraction determined for Q10. Thus, for IMM samples with a lipid:solanesol mixing ratio of 25:1, the solanesol proportion was estimated to be ~1.5 mol%.

3.2.2. Effect of Q10 and solanesol on lipid chain order

In order to probe the lipid chain order the steady-state anisotropy of DPH was measured in IMM samples supplemented with either Q10 or solanesol. The results from these experiments are summarized in Fig. 3, which for comparison also include data reported previously for POPC liposomes [18]. As evident from the significant increase in fluorescence anisotropy, the IMM model membrane becomes more ordered in the presence of Q10. It is worth noting that the magnitude of the anisotropy increase is similar to that observed in the POPC system, suggesting that Q10 has a comparable effect in both systems. The insignificant effect of solanesol on the anisotropy suggests that the quinone ring plays a relevant role in the ordering of the membrane also in case of the IMM model membranes. The different results observed for Q10 and solanesol

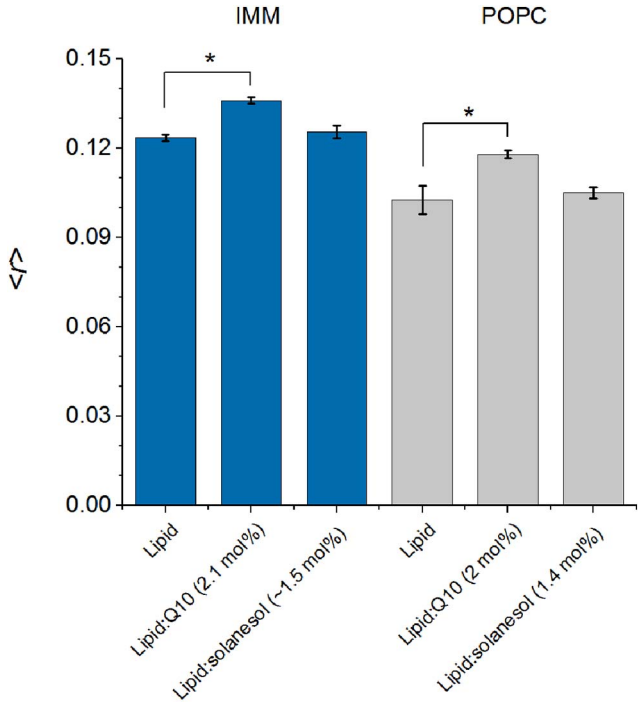

Fig. 3. The effect of Q10 and solanesol on the DPH fluorescence anisotropy for the IMM and the POPC system at 25 °C. Data for POPC and POPC:Q10 are from reference [18]. The proportion of Q10 or solanesol in the membrane is indicated in parenthesis. *Indicates a significant difference according to an unpaired *t*-test at a 95% confidence level.

indicate that the Q10 molecule resides in the membrane, at least partially, with the quinone moiety located close to the lipid headgroups. In summary, the results displayed in Fig. 3 show that Q10 exerts a significant ordering effect in the IMM model membranes, and that the mechanism giving rise to this effect likely is the same as in the less complex POPC model.

3.2.3. *Spreading of liposomes onto silica surfaces*

By following the adhesion and eventual spreading of liposomes onto silica surfaces it is possible to obtain a qualitative measure of the resistance of the lipid membrane towards deformation and rupture. Loading of liposomes onto a silica substrate can result in either the formation of an immobilized layer of intact liposomes or rupture of the liposomes, followed by the formation of a supported lipid bilayer. The outcome depends mainly on the mechanical stability of the liposomes themselves (more stable liposomes are less prone to rupture) and on the strength of the membrane-silica interaction (stronger attraction leads to higher probability of rupture). It has in addition been suggested that the strength of liposome-liposome interactions may play a role in cases where a critical concentration of liposomes needs to be reached on the surface for the rupture to occur [37].

The behaviour of IMM liposomes on a silica substrate was followed with the help of the QCM-D. In the QCM-D experiments, shifts in oscillation frequency (Δf) and dissipation factor (ΔD) of a silica-coated quartz sensor are measured. These shifts are coupled to the properties of the attached film on the sensor surface. Negative frequency shifts relate to an adsorbed mass, while shifts in the dissipation factor correspond to changes in the viscoelastic properties at the interface [38]. When the adsorbed material forms a thin rigid film, the dissipation factor remains unchanged ($\Delta D = 0$), and the adsorbed surface mass density can be easily calculated using the Sauerbrey relationship:

$$m = -C\Delta f_n n^{-1} \quad (4)$$

where C is the mass sensitivity constant (17.7 ng cm^{-2} Hz^{-1} for the experimental setup used), Δf_n the measured frequency shift, and n the overtone number. This relationship is expected to be valid when liposomes rupture and spread on a surface, forming a supported lipid bilayer [39]. If a layer of intact liposomes is formed instead, the change in dissipation factor is expected to be much larger than zero.

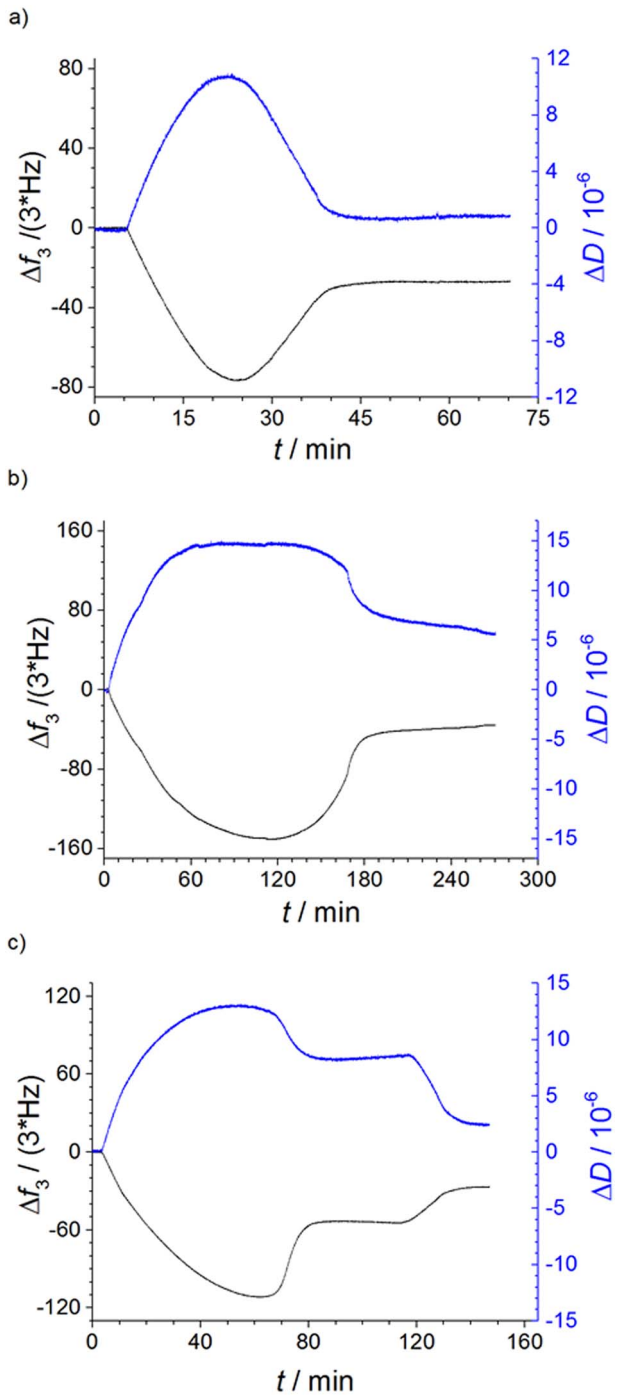

Fig. 4. QCM-D (3rd overtone) data showing the adhesion and spreading on silica of a) IMM, b) IMM:Q10 (mixing ratio 25:1), and c) IMM:solanesol (mixing ratio 25:1) liposomes.

The results shown in Fig. 4 suggest that both IMM and IMM:solanesol liposomes attach and spread onto the silica surface (final $\Delta D \sim 0$). In the latter case, intact liposomes still remain on the surface after the initial rupture and spreading event, but they are removed upon rinsing, suggesting that they are not directly attached to the surface, but are situated on top of the formed supported lipid bilayer. IMM:Q10 liposomes, on the other hand, attach and only spread partially, resulting

in intact liposomes remaining on the surface even after prolonged rinsing ($\Delta D > 0$). For the first two cases, the surface mass densities of the adsorbed films can be calculated using Eq. (4). The obtained values are 488 ng/cm^2 for IMM and 528 ng/cm^2 for IMM:solanesol. This can be compared to 452 ng/cm^2 for POPC [18].

From these results it can be concluded that the IMM model membrane is not only more ordered, but also denser than the pure POPC membrane. The denser membrane could partly be due to tighter packing of the lipids, resulting from strong attractive forces between the lipid headgroups, e.g. hydrogen bonding between the PE headgroups [40]. The fact that solanesol induces an additional increase in membrane density is interesting. A similar effect was previously seen with POPC membranes, although the increase was marginal. Taken together the results suggest that solanesol has a slight condensing effect on lipid membranes, albeit this does not translated into a higher degree of lipid order or a noticeable higher resistance to membrane rupture.

The density for the Q10 supplemented IMM-based lipid bilayer could not be calculated, since the liposomes only partially spread on the surfaces. The incomplete spreading indicates, however, that the inclusion of Q10 results in a membrane that is more resistant towards rupture; in other words, Q10 appears to increase the mechanical stability of the IMM membrane.

3.2.4. Spontaneous and surfactant induced leakage

To elucidate whether the increased lipid packing order observed in the presence of Q10 translates into improved membrane barrier properties, we carried out a series of experiments in which the leakage of encapsulated CF from the liposomes was monitored. From the results shown in Fig. 5, it can be seen that CF is spontaneously released at a slower rate from IMM-liposomes compared to POPC-liposomes. Adding Q10 into the membrane further decreases the rate of leakage. These findings are in agreement with the assumption that a decreased leakage rate is coupled to an increased degree of lipid order. Interestingly, however, introducing solanesol into the membrane has roughly the same effect on the spontaneous leakage rate as that obtained by including Q10. It is therefore apparent that, in contrast to what has been observed for POPC membranes, the mechanism behind the reduced permeability cannot simply be traced back to a higher degree of lipid packing order.

To complement the above experiments, a study of surfactant promoted leakage was performed. The results displayed in Fig. 6a show that the surfactant induced leakage follows the same trend as that observed in case of the spontaneous leakage, i.e. the CF is released more slowly in systems containing Q10 or solanesol. This observation further supports the lack of a direct connection between the degree of lipid packing order and the barrier properties of the IMM membrane. Further, given that both solanesol and Q10 have a similar effect, the results imply that the quinone headgroup of the latter is not vital to reduce the leakage rate. This suggests that the CF leakage can be modulated and decreased via a mechanism that involves primarily the isoprenoid unit, i.e., a long hydrophobic hydrocarbon chain. To test this hypothesis we investigated the surfactant-induced leakage of CF from IMM liposomes supplemented with hexadecane (a cryo-TEM picture of these liposomes is found in Fig. S3 in the Supplementary Material). As shown by the results presented in Fig. 6a, inclusion of 7 mol% hexadecane in the liposomal preparations resulted, as expected, in a clearly reduced rate of CF release.

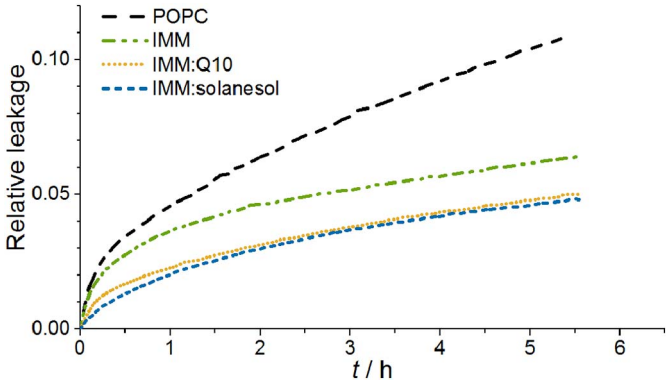

Fig. 5. Representative spontaneous leakage profiles of carboxyfluorescein from liposomes with different compositions, at 25 °C. The mixing ratio of IMM lipids with Q10 and solanesol, respectively, is 25:1.

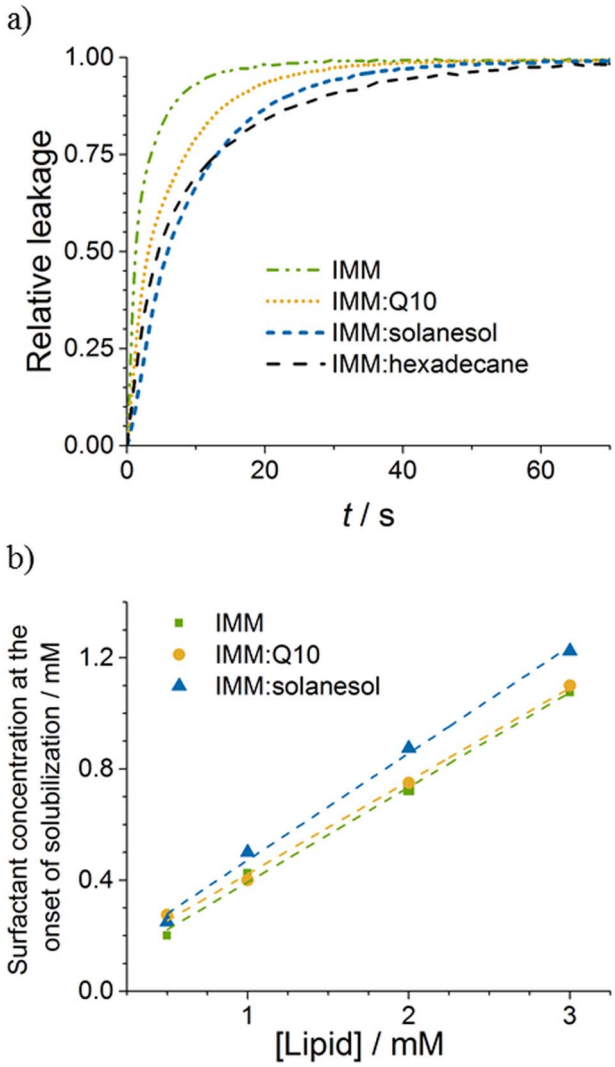

Fig. 6. a) Surfactant mediated leakage from IMM-liposomes at 67.5 μM $C_{12}E_8$ and b) the correlation between the lipid concentration and the surfactant concentration at the onset of solubilisation for IMM liposomes, both at 25 °C. Mixing ratios: IMM:Q10 25:1, IMM:solanesol 25:1, and IMM:hexadecane 13:1.

The reduced leakage observed in the presence of Q10 and solanesol could, in theory, originate from a reduced propensity of the surfactant $C_{12}E_8$ to distribute from the aqueous phase into the liposome membranes. To rule out this possibility, we investigated the partition behaviour of $C_{12}E_8$ in the IMM, IMM:Q10, and IMM:solanesol liposome systems (see Section 2.6 for details). Using the data presented in Fig. 6b, the membrane/buffer partition coefficients values were calculated to 3.39 ± 0.11 mM^{-1} for IMM, 3.34 ± 0.09 mM^{-1} for IMM:Q10 (25:1 mixing ratio) and 3.70 ± 0.12 mM^{-1} for IMM:solanesol (25:1 mixing ratio). The differences between the obtained values are negligible when related to the precision of the experiments; in fact, the estimated membrane-bound surfactant concentrations are roughly the same in all three systems.

Summarizing, we can conclude that, in agreement with the results obtained with pure POPC liposomes, the permeability of the IMM model membrane towards small hydrophilic molecules decreases upon incorporation of Q10. However, and in contrast to previous conclusions drawn from the POPC system, this effect is observed regardless of whether the quinone moiety is present or not. Thus, in the IMM, but not the POPC system, the long hydrophobic chain appears sufficient to decrease the leakage.

3.2.5. Possible coupling between membrane location and effect of Q10

The results presented in the previous sections indicate some important differences between the properties of the POPC and IMM model membranes, and possibly also their interaction with Q10. Given the observed tight lipid packing and high membrane density, it's plausible to assume that the IMM model membrane contains components that, either alone or in concert, affect both the location and the effect of Q10 in the membrane. In support of this assumption, recent studies have shown that the position of the quinone ring of Q10 can vary depending on the lateral pressure in the membrane. Results from monolayer studies reveal, e.g., that Q10 is completely expelled from the headgroup region at large film pressures [21,41]. It is thus possible that in the comparably more dense and ordered IMM, a significant proportion of the Q10 molecules are fully immersed deeply in the hydrophobic region of the membrane, while only a fraction remains with the quinone moiety close to the headgroup region (accounting thus for the increase in lipid order). This assumption is further supported by previous molecular dynamics simulations, in which the quinone ring was shown to reside close to the PC headgroups in POPC membranes [20], while in a mitochondria-mimicking membrane a large proportion of the ubiquinone molecules resided exclusively in the center of the membrane [19]. In this scenario, the effect of Q10 on the CF leakage from the IMM liposomes would be very similar to that of the more or less purely hydrophobic molecule solanesol. The reason why the presence of Q10/solanesol in the hydrophobic part of the IMM membrane tends to reduce the CF leakage remains, however, an unresolved question. It can be speculated that the effect is related to the presence of an inherent curvature elastic stress in the IMM model membrane. The IMM model contains two lipids, POPE and CL, with negative spontaneous curvature and a propensity to form structures with negative curvature [42]. In other words, there is an energy cost associated with forcing POPE and CL lipids into structures of positive, or even zero curvature. A further increase in the negative curvature stress is anticipated upon inclusion of large molecules, such as Q10, or solanesol, that reside in the hydrophobic part of the membrane. Since the leakage of CF takes place mainly through transient pores [43,44], i.e., structures of high positive curvature, that form spontaneously in the membrane, it appears reasonable that factors promoting negative curvature strain would supress the leakage rate. In case of POPC membranes there is no intrinsic negative curvature stress, and the addition of solanesol exerts no reducing effect on either spontaneous or surfactant induced CF leakage [18]. The strong effect observed upon inclusion of Q10 in pure POPC membranes originates instead most likely from the membrane condensing effect, which tends to reduce the prevalence and/or lifetime of transient pores. In case of the fluid and disordered POPC membrane, the Q10-induced increase in lipid packing order and membrane density obviously has an important impact on the membrane permeability, while a marginal increase in the hydrophobic volume resulting from inclusion of solanesol has no significant effect.

In order to further investigate and explain the differences observed between IMM and POPC liposomes, we conducted additional experiments with the aim to explore the role of the different components in the IMM mixture. Thus, with the exception of the minor PI and PS constituents, the various lipid components were studied independently and in simplified two-component mixtures.

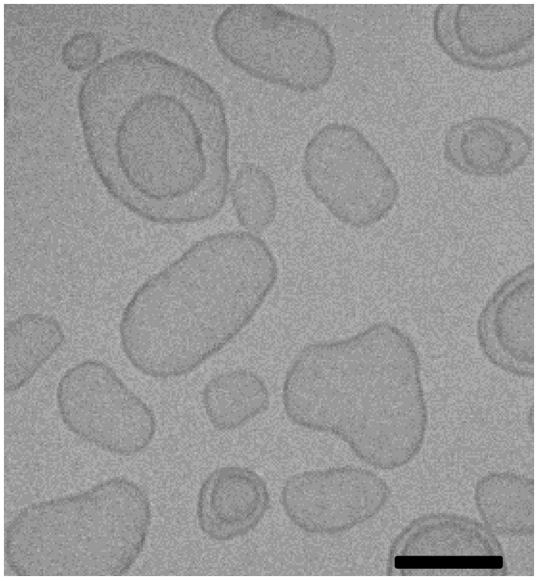

Fig. 7. Cryo-TEM micrograph of cardiolipin (CL) liposomes at 25 °C. The scalebar is 100 nm.

3.3. Role of specific phospholipids in the IMM mimetics

3.3.1. CL – a peculiar lipid in the IMM composition

Cardiolipins constitute a special class of lipids where two phosphate groups, each bound to two acyl chains, are linked together at the opposite ends of a common glycerol backbone. At physiological conditions the lipids have a double negative charge [45]. Since the phosphate groups are tightly connected to each other, and the four lipid chains make up for a very bulky hydrophobic moiety, there is a tendency for CL to form inverted structures. However, lamellar structures have often been observed upon suspension of CL in buffers mimicking physiological conditions [46,47], likely because of a strong electrostatic repulsion between the headgroups of different molecules. At certain solution conditions, such as high ionic strengths or low pH, the electrostatic repulsion between headgroups is diminished and structures with negative curvature can be formed [42,48–50]. Also, the degree of acyl chain saturation affects the phase structure, with unsaturations in the acyl chains favoring the formation of inverted structures [51].

As revealed by the micrograph displayed in Fig. 7, CL derived from bovine heart formed liposomes when treated according to the preparation protocol described in Section 2.2. By comparison with Fig. 2 it can be seen, however, that the liposomes display an irregular, non-spherical shape, suggesting that the membrane is very soft, having a low bending and compressibility modulus. The very fluid nature of the membranes is further corroborated by the results from fluorescence anisotropy measurements, which show a drastically reduced lipid order compared to POPC (Fig. 8) [18]. These results are in line with fluorescence correlation spectroscopy experiments performed by J. Unsay et al. [52] in which CL was shown to increase the membrane fluidity in PC-based membranes. As displayed in Fig. 8, incorporation of Q10 into the CL membrane increased the lipid order, and, noteworthy, at the lipid:Q10 mixing ratio used (25:1), all of the added Q10 was found to be included in the membrane. Addition of solanesol, on the other hand, distinctly decreased the degree of order in the membrane. The ordering effect of Q10 agrees with the previous findings with POPC and IMM model membranes, suggesting that it could be a general effect of Q10 regardless of the membrane composition. The disordering effect noted for solanesol appears, in contrast, to be more specific, since this effect was not observed for neither POPC nor IMM membranes. Notably, inclusion of solanesol in liposomes composed of a mixture of POPC and CL (94:6 M ratio) (Fig. 8) did not lead to any significant changes in the

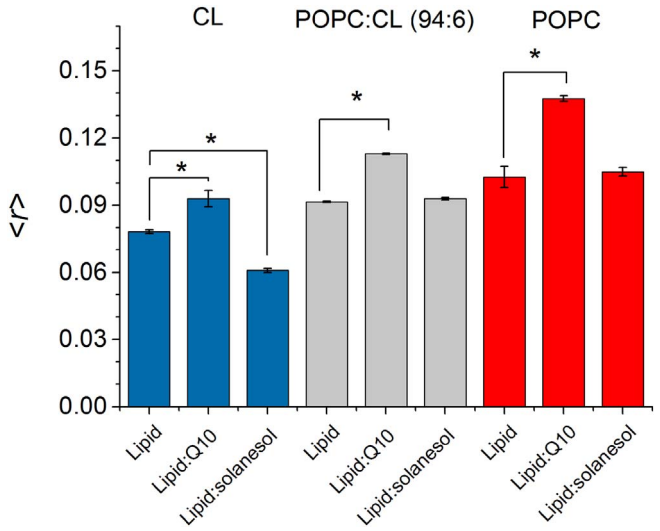

Fig. 8. The effect of Q10 and solanesol on the DPH fluorescence anisotropy for the CL-. POPC:CL (94:6) and POPC-based systems at 25 °C. The lipid:Q10 and lipid:solanesol mixing ratio is 25:1 in all cases* Indicates a significant difference according to an unpaired *t*-test at a 95% confidence level. POPC data are taken from reference [18].

fluorescence anisotropy. This indicates that the disordering effect of solanesol is observed only for either extremely soft or significantly curvature strained membranes. Some further insights regarding this matter were gained from the experiments using POPE-based liposomes described in next section.

3.3.2. *POPE – A dominant lipid species in the IMM composition*

The main component in the IMM mixture is POPE, a lipid that has an even stronger tendency than CL to form structures with negative curvature [42,53]. Hydration, followed by freeze-thawing of the pure POPE lipid films resulted in suspensions that flocculated immediately, producing large aggregates visible to the naked eye (Fig. S4a in the supplementary material). After extrusion at 37 °C, the initially clear suspension rapidly became turbid, and inspection by optical microscopy revealed the presence of large particles (Fig. S4b). This behaviour suggests either the formation of non-lamellar structures, or fast liposome aggregation. Cryo-TEM investigations showed that the latter hypothesis is correct, as large clusters of tightly aggregated liposomes, but no non-lamellar structures, could be observed in the micrographs (see Fig. S5 in the supplementary material). The strong tendency for aggregation indicates that the POPE liposomes are very rigid, leading to a decrease in the thermal fluctuations that usually keep softer liposomes in suspension. The high rigidity of the POPE membranes most likely originates from the strong hydrogen bonding between the PE headgroups [40,54].

The formation of flocks and the subsequent sedimentation of the lipid particles prevented further investigations of the pure POPE system. In order to achieve stable POPE liposomes, a small amount of cerPEG(5000) (0.25 mol%) [55] was included in the POPE sample to provide the liposomes with steric stabilization. As expected, the PEG-stabilized liposomes had a much lower tendency to aggregate and could be better characterized with cryo-TEM. The obtained micrographs are shown in Fig. 9a. Liposomes composed of a mixture of POPE and POPC at a ratio similar to the one found in the IMM (POPE:POPC, 1:1) were also prepared and investigated by means of cryo-TEM (Fig. 9b). Both types of liposomes showed a certain tendency to aggregate over time, although the suspensions were stable for several hours, allowing thus for further experiments.

Measurements of the DPH fluorescence anisotropy in the PEG-stabilized POPE, POPC:POPE, as well as pure POPC samples were performed at 30 °C in order to ensure that the lipid membranes were all in the liquid crystalline phase state (POPE has a T_m corresponding to

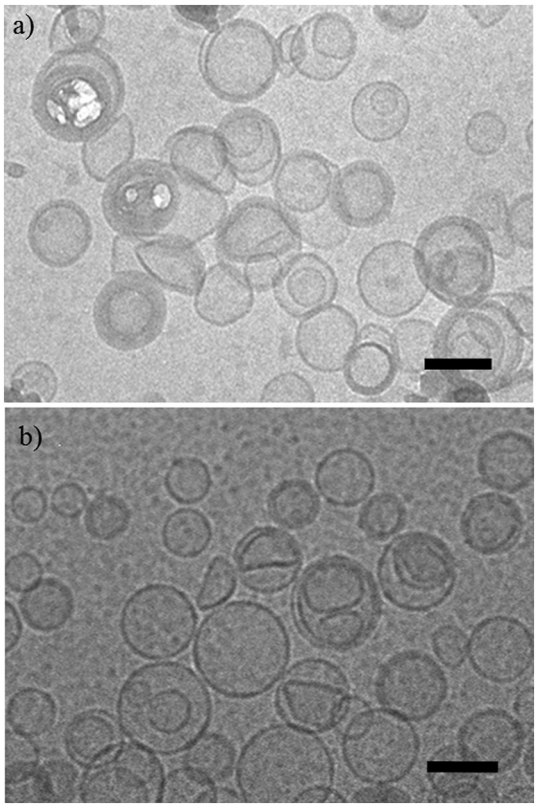

Fig. 9. Cryo-TEM micrographs of a) POPE:cerPEG5000 (100:0.25) at 37 °C liposomes and b) POPC:POPE (1:1) liposomes at 25 °C. The scale bar is 100 nm.

~25 °C [56]). The results, which are summarized in Fig. 10a, confirm a considerably higher lipid chain order in the POPE compared to the POPC membranes, and show that POPE, in contrast to CL, tends to increase the packing order when included in POPC membranes. The observed differences in lipid packing order between the pure POPC and POPE membranes agrees with previously reported order parameters determined by deuterium NMR experiments [57]. The reason for the higher packing order in the POPE membranes can partly be traced back to the negative spontaneous curvature of POPE, which couples to a need for the hydrocarbon chains to stretch and pack tightly upon formation of a flat lipid bilayer.

In a next step, we investigated the effect of Q10 on the lipid packing order in the POPE membranes. Noteworthy, analyses based on the method described in Section 2.4 revealed that the liposomes incorporated an even lower fraction of the added Q10 than what was determined in case of the IMM liposomes. Thus, the final Q10 proportion in the membrane was in this case found to be 1.6 mol%. In order to probe possible differences due to variations in membrane fluidity, the experiments were carried out at both 30 and 37 °C. Measurements were in parallel also performed with solanesol-supplemented liposomes. As shown in Fig. 10b, solanesol had, similar to what was observed in case of CL liposomes, a significant disordering effect on the membranes at all tested temperatures. The fact that both the soft CL and the rigid POPE membranes become more fluid in the presence of solanesol, while POPC membranes remain unaffected, indicates that the disordering effect occurs in connection with an inherent negative curvature stress in the membrane. Noteworthy, in case of experiments performed at 30 °C a tendency towards more disordered membranes was observed also upon inclusion of Q10 in the POPE membranes (Fig. 10b). The data thus suggest that Q10 and solanesol both have a fluidizing effect in POPE membranes. As discussed above, POPE membranes are rigid in nature, and the lateral pressure is rather high, particularly in the headgroup area where hydrogen bonding keeps the headgroups tightly bound

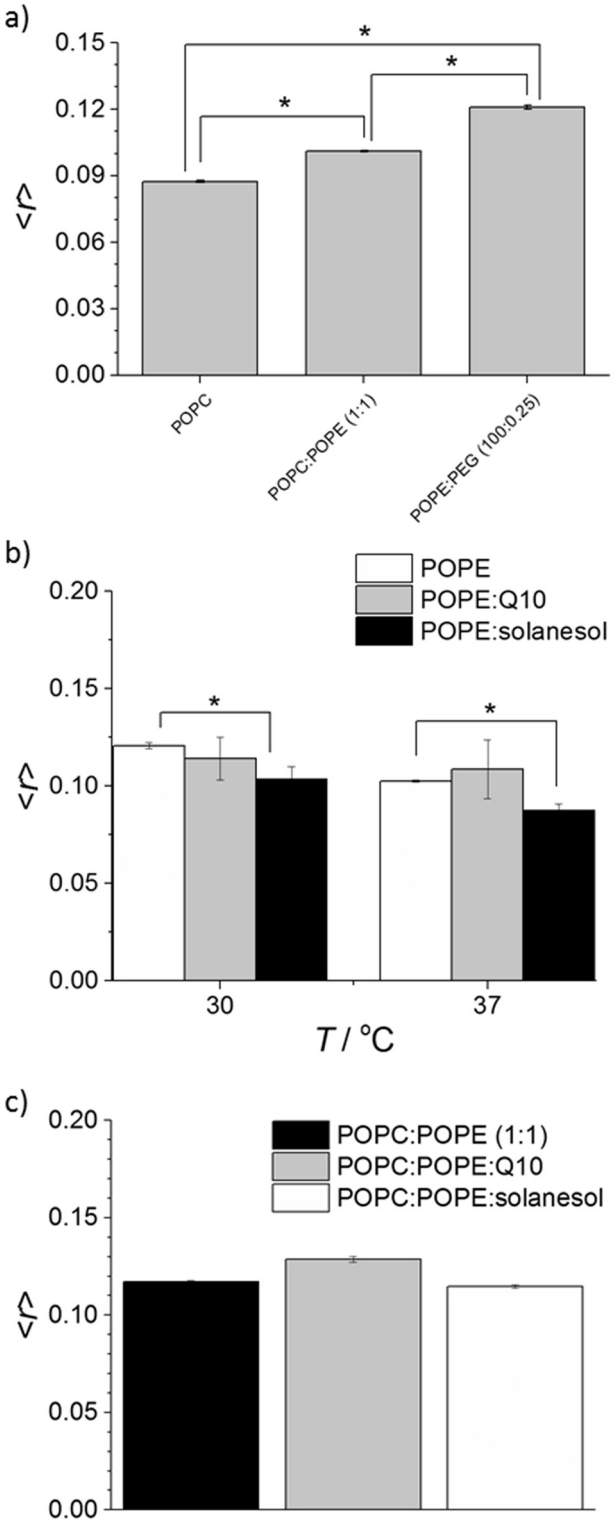

Fig. 10. Fluorescence anisotropy data for a) POPC, POPC:POPE (1:1) and POPE:cerPEG5000 (100:0.25) at 30 °C, b) the POPE, POPE:Q10 and POPE:solanesol (25:1 mixing ratios) systems at different temperatures, and c) the POPC:POPE (1:1) system at 25 °C upon inclusion of Q10 or solanesol (25:1 mixing ratios). * Indicates a significant difference according to an unpaired *t*-test at a 95% confidence level.

together. At this high lateral pressure it can be foreseen that most of the added Q10 will be located deeply within the hydrophobic part of the membrane, in a fashion similar to what is expected for solanesol. This prediction is in agreement with previous reports suggesting that ubiquinones are partially excluded from the headgroup region of PE [58] and PE-rich membranes [19]. As a consequence of their deep location in the membrane, both Q10 and solanesol exert a disordering effect, presumably by impeding close packing of the hydrocarbon chains in the mid-region of the membrane. The weaker disordering effect of Q10 than of solanesol in POPE membranes is probably due to the fact that a small fraction of the total Q10 content is located with the quinone moiety near the headgroup area, thus counteracting the disordering effect. The probability that Q10 assumes this orientation in the membrane can be expected to vary with changes in conditions that affect the membrane fluidity, such as temperature. In line with this, data displayed Fig. 10b indicate that Q10 actually has a slight ordering effect on the membrane when the temperature is increased to 37 °C.

Notably, as shown in Fig. 10c, membranes composed of an equimolar mixture of POPC and POPE interact with Q10 and solanesol in a manner closer to what is observed with pure POPC and with IMM membranes. In this case the lateral pressure is obviously low enough to allow a considerable fraction of the Q10 to reside in the headgroup region, and thereby cause an overall increase in the lipid packing order.

The low long-term stability of the POPE preparations prevented us from complementing the anisotropy data with leakage experiments. Instead, the detergent induced leakage from the POPC:POPE (1:1) system was measured. As can be seen in Fig. 11, the results follow the same trend as in the IMM model system, i.e., both Q10 and solanesol decrease the rate of detergent induced leakage, with the latter being more effective. Similar to in the IMM system, it can thus be concluded that the leakage reducing effect of solanesol does not correlate with an increased degree of order in the membrane. The similarity of the trends observed in the POPC:POPE and IMM systems suggest that the properties of the IMM model membrane are largely defined by the presence of substantial amounts of POPE. The fact that the surfactant induced leakage is slower from the IMM than the POPC:POPE liposomes shows, however, that the IMM mixture contains additional components, such as CL, that tend to further improve the barrier properties.

In order to further verify the central role of POPE, we investigated the surfactant induced leakage in a simplified IMM-model, in which POPE was replaced with POPC (POPC:CL:POPS, 92.2: 6.1: 1.7). As shown in Fig. 12, the leakage was in this case determined to be almost as fast as from the pure POPC liposomes, and, importantly, Q10 had a more pronounced leakage reducing effect than solanesol. The latter finding confirms that the presence of POPE is required in order for solanesol to exert a leakage reducing effect that is similar to, or stronger than that of Q10.

From the data presented in Fig. 12 it may be noted that the surfactant-induced leakage is slightly slower from the POPE depleted IMM

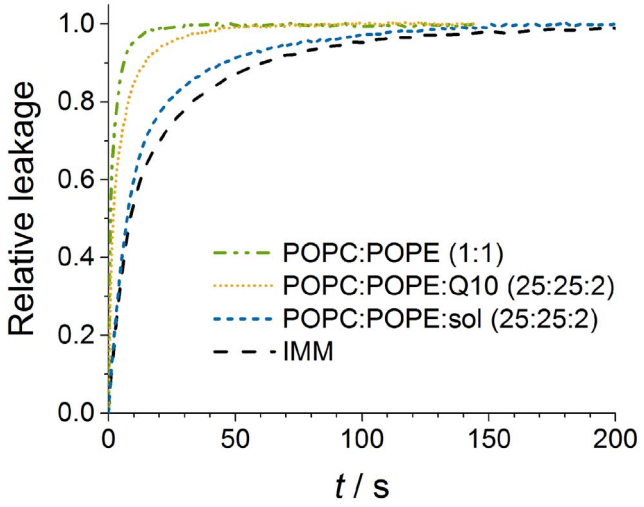

Fig. 11. Surfactant mediated leakage at 62.5 μM $C_{12}E_8$ for different compositions at 25 °C. Compositions are shown as molar mixing ratios.

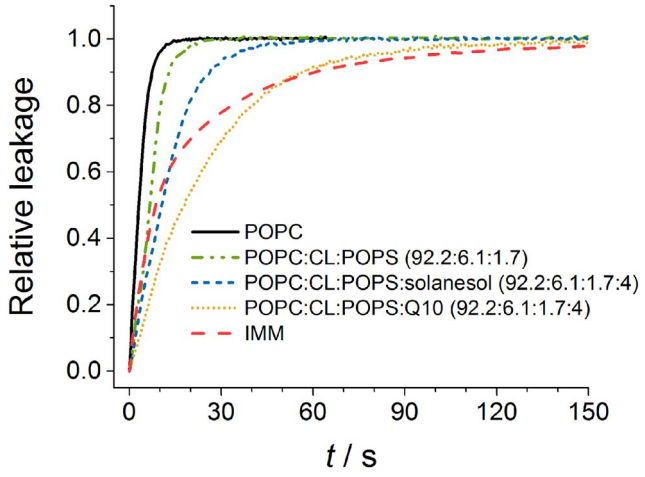

Fig. 12. Surfactant mediated leakage at 62.5 μM $C_{12}E_8$ for different lipid compositions at 25 °C. Compositions are given in terms of molar mixing ratios.

liposomes, as compared to the pure POPC liposomes. This indicates that CL, the second major component in the mixture, provides with increased resistance towards detergent action. As discussed in Section 3.2.4, a probable explanation for this is that CL introduces a negative curvature strain in the membrane, which in turn reduces the occurrence of positively curved pores and defects in the membrane.

4. Summary and concluding remarks

The data reported in the present study show that ubiquinone-10 (Q10) increases the lipid packing order and the mechanical stability, and improves the barrier properties of the investigated IMM-mimicking membranes. It can thus be concluded that Q10, in these respects, has a membrane stabilizing effect that is similar to that previously observed in pure POPC membranes [18]. Some interesting and important differences were discovered, however, between the two systems. The observation that solanesol is as effective as Q10 in reducing CF leakage, while it has no significant effect on the lipid packing order, shows that the barrier properties are not directly correlated to the fluidity of the IMM-mimicking membranes. A mechanism other than increased lipid order must be responsible for the leakage reducing effect of solanesol. Since solanesol lacks effect in pure POPC membranes, this mechanism is obviously dependent on the inherent properties of the IMM-mimicking membrane, as defined by its lipid composition. Based on the experimental evidence collected in the present work, it appears plausible that solanesol reduces the CF leakage by amplifying the intrinsic curvature elastic stress in the IMM membrane. More specifically, the presence of solanesol in the hydrophobic region leads to an increased negative curvature strain that counteracts formation of the membrane pores and defects responsible for CF leakage. Reasoning along these lines has been used previously to explain why negative curvature-inducing lipids inhibit the peptide-induced release of calcein and CF from liposomes [59–61]. It is conceivable that a corresponding mechanism also contributes to, and perhaps even dominates, the leakage reducing effect observed for Q10 in the IMM-mimicking membranes. As a consequence of the inherent curvature elastic stress and, in particular, the effective hydrogen bonding between PE-PE, and likely also PE-CL and PE-PC, headgroups [40,54,58], the lateral pressure in the headgroup region of the IMM-mimicking membrane is comparatively high. Under these conditions only part of the added Q10 appears to be located with the quinone moiety close to the headgroup region, while the rest assumes a membrane location similar to that of solanesol. Although further investigations by, e.g., NMR and IR spectroscopy are needed to more precisely determine the distribution and location of Q10 in the membrane, it is clear that POPE plays a key role in modulating and governing Q10's interaction with the IMM model membrane.

A natural next step towards learning more about Q10's possible stabilizing function in the inner mitochondrial membrane would be to further improve the model membrane. Complementary future studies should focus on, e.g., the role of the acyl chains (length and degree of saturation), which was only partially considered in the present study. It is moreover important to remark that the inner mitochondrial membrane has a very high load of proteins. About 80% of the dry weight of the inner mitochondrial membrane mass consists of proteins, of which approximately one half corresponds to integral membrane proteins while the rest are peripheral [62]. The high protein content can be expected to lead to lipid segregation and other processes that impact the overall membrane structure and dynamics [63–67]. Besides ubiquinone, there are also other lipophilic molecules in the inner membrane of the mitochondria that could affect the membrane properties, by themselves or possibly in synergy with Q10. For example, α-tocopherol and its derivatives have been shown to modify the properties of lipid membranes [68]. Q10 itself, in its reduced form, should also be investigated, as it is likely that the hydroquinone group will have a particularly strong tendency to sit near the lipid headgroups [69,70]. In conclusion there are several aspects of the mitochondrial membrane that need to be investigated and clarified in order to gain a deeper understanding of the membrane stabilizing effect of ubiquinone-10. The findings reported in the present study constitute, however, an important step towards a more integral understanding of the role of the different components of the mitochondrial membrane.

Transparency document

The Transparency document associated with this article can be found, in online version.

Acknowledgments

Financial support from the Swedish Research Council (2016-03464) and the Swedish Cancer Society (17 0566) is gratefully acknowledged. Cristian Hartman, Simonne Jocic and Marius Markenstein are gratefully acknowledged for assistance with the experimental work. We also thank Dr. Jonny Eriksson (Department of Chemistry-BMC, Uppsala University) for help with the Cryo-TEM experiments and Dr. Denny Mahlin (Department of Pharmacy, Uppsala University) for valuable assistance with complementary DSC measurements. The POPC material was a kind gift from Lipoid Gmbh, Ludwigshafen, Germany.

Appendix A. Supplementary data

Supplementary data to this article can be found online at https://doi.org/10.1016/j.bbamem.2018.02.015.

References

[1] F.L. Crane, Y. Hatefi, R.L. Lester, C. Widmer, Isolation of a QUINONE from beef heart mitochondria, Biochim. Biophys. Acta 25 (1957) 220–221.
[2] M.D. Collins, D. Jones, Distribution of isoprenoid quinone structural types in bacteria and their taxonomic implication, Microbiol. Rev. 45 (1981) 316.
[3] Y. Hatefi, A.G. Haavik, L.R. Fowler, D.E. Griffiths, Studies on the electron transfer system: XLII. Reconstitution of the electron transfer system, J. Biol. Chem. 237 (1962) 2661–2669.
[4] A. Kroger, M. Klingenberg, S. Schweidl, Kinetics of redox reactions of ubiquinone related to electron-transport activity in respiratory chain, Eur. J. Biochem. 34 (1973) 358–368.
[5] A. Kroger, M. Klingenberg, Further evidence for pool function of ubiquinone as derived from inhibition of electron-transport by antimycin, Eur. J. Biochem. 39 (1973) 313–323.
[6] L. Ernster, G. Dallner, Biochemical, physiological and medical aspects of ubiquinone function, Biochim. Biophys. Acta Mol. basis Dis. 1271 (1995) 195–204.
[7] B. Frei, M.C. Kim, B.N. Ames, Ubiquinol-10 is an effective lipid-soluble antioxidant at physiological concentrations, Proc. Natl. Acad. Sci. 87 (1990) 4879–4883.
[8] F.L. Crane, New functions for coenzyme Q, Protoplasma 213 (2000) 127–133.
[9] R. Alleva, M. Tomasetti, L. Andera, N. Gellert, B. Borghi, C. Weber, M.P. Murphy,

J. Neuzil, Coenzyme Q blocks biochemical but not receptor-mediated apoptosis by increasing mitochondrial antioxidant protection, FEBS Lett. 503 (2001) 46–50.
[10] T. Kagan, C. Davis, L.I.N. Lin, Z. Zakeri, Coenzyme Q10 can in some circumstances block apoptosis, and this effect is mediated through mitochondria, Ann. N. Y. Acad. Sci. 887 (1999) 31–47.
[11] M. Turunen, J. Olsson, G. Dallner, Metabolism and function of coenzyme Q, Biochim. Biophys. Acta Biomembr. 1660 (2004) 171–199.
[12] M. Bentinger, M. Tekle, G. Dallner, Coenzyme Q – biosynthesis and functions, Biochem. Biophys. Res. Commun. 396 (2010) 74–79.
[13] J. Garrido-Maraver, M.D. Cordero, M. Oropesa-Ávila, A. Fernández Vega, M. De La Mata, A. Delgado Pavón, M. De Miguel, C. Pérez Calero, M. Villanueva Paz, D. Cotán, Coenzyme Q10 therapy, Molecular Syndromology, 5 2014, pp. 187–197.
[14] U. Cobanoglu, H. Demir, A. Cebi, F. Sayir, H.H. Alp, Z. Akan, T. Gur, E. Bakan, Lipid peroxidation, DNA damage and coenzyme Q10 in lung cancer patients—markers for risk assessment? Asian Pac. J. Cancer Prev. 12 (2011) 1399–1403.
[15] K. Folkers, A. Osterborg, M. Nylander, M. Morita, H. Mellstedt, Activities of vitamin Q 10 in animal models and a serious deficiency in patients with cancer, Biochem. Biophys. Res. Commun. 234 (1997) 296–299.
[16] D.C. Sevin, U. Sauer, Ubiquinone accumulation improves osmotic-stress tolerance in *Escherichia coli*, Nat. Chem. Biol. 10 (2014) (266-+).
[17] C.F. Clarke, A.C. Rowat, J.W. Gober, Osmotic stress: is CoQ a membrane stabilizer? Nat. Chem. Biol. 10 (2014) 242–243.
[18] V. Agmo Hernández, E.K. Eriksson, K. Edwards, Ubiquinone-10 alters mechanical properties and increases stability of phospholipid membranes, Biochim. Biophys. Acta Biomembr. 1848 (2015) 2233–2243.
[19] P. Kaurola, V. Sharma, A. Vonk, I. Vattulainen, T. Róg, Distribution and dynamics of quinones in the lipid bilayer mimicking the inner membrane of mitochondria, Biochim. Biophys. Acta Biomembr. 1858 (2016) 2116–2122.
[20] V.V. Galassi, G.M. Arantes, Partition, orientation and mobility of ubiquinones in a lipid bilayer, Biochim. Biophys. Acta Bioenerg. 1847 (2015) 1560–1573.
[21] W. Nerdal, T.R.S. Nilsen, S. Steinkopf, CoenzymeQ(10), localizations in model membranes. A Langmuir monolayer study, Biophys. Chem. 207 (2015) 74–81.
[22] N. Heise, F. Scholz, Assessing the effect of the lipid environment on the redox potentials of the coenzymes Q10 and Q4 using lipid monolayers made of DOPC, DMPC, TMCL, TOCL, and natural cardiolipin (nCL) on mercury, Electrochem. Commun. 81 (2017) 141–144.
[23] S. Fleischer, G. Rouser, B. Fleischer, A. Casu, G. Kritchevsky, Lipid composition of mitochondria from bovine heart, liver, and kidney, J. Lipid Res. 8 (1967) 170–180.
[24] F. Åberg, Y. Zhang, H. Teclebrhan, E.-L. Appelkvist, G. Dallner, Increases in tissue levels of ubiquinone in association with peroxisome proliferation, Chem. Biol. Interact. 99 (1996) 205–218.
[25] R. Hovius, H. Lambrechts, K. Nicolay, B. de Kruijff, Improved methods to isolate and subfractionate rat liver mitochondria. Lipid composition of the inner and outer membrane, Biochim. Biophys. Acta Biomembr. 1021 (1990) 217–226.
[26] V. Agmo Hernández, G. Karlsson, K. Edwards, Intrinsic heterogeneity in liposome suspensions caused by the dynamic spontaneous formation of hydrophobic active sites in lipid membranes, Langmuir 27 (2011) 4873–4883.
[27] M. Almgren, K. Edwards, G. Karlsson, Cryo transmission electron microscopy of liposomes and related structures, Colloids Surf. A Physicochem. Eng. Asp. 174 (2000) 3–21.
[28] J.V. Paraskova, E. Rydin, P.J.R. Sjöberg, Extraction and quantification of phosphorus derived from DNA and lipids in environmental samples, Talanta 115 (2013) 336–341.
[29] A. Kroger, Determination of contents and redox states of ubiquinone and menaquinone, Methods Enzymol. 53 (1978) 579–591.
[30] R.D. Kaiser, E. London, Location of diphenylhexatriene (DPH) and its derivatives within membranes: comparison of different fluorescence quenching analyses of membrane depth, Biochemistry 37 (1998) 8180–8190.
[31] M. Silvander, P. Hansson, K. Edwards, Liposomal surface potential and bilayer packing as affected by PEG − lipid inclusion, Langmuir 16 (2000) 3696–3702.
[32] M. Johnsson, K. Edwards, Interactions between nonionic surfactants and sterically stabilized phophatidyl choline liposomes†, Langmuir 16 (2000) 8632–8642.
[33] F.M. Ruggiero, C. Landriscina, G.V. Gnoni, E. Quagliariello, Lipid composition of liver mitochondria and microsomes in hyperthyroid rats, Lipids 19 (1984) 171–178.
[34] R.E. Dale, L.A. Chen, L. Brand, Rotational relaxation of the “microviscosity” probe diphenylhexatriene in paraffin oil and egg lecithin vesicles, J. Biol. Chem. 252 (1977) 7500–7510.
[35] H.-T. Cheng, Megha and London, E., Preparation and properties of asymmetric vesicles that mimic cell membranes: effect upon lipid raft formation and transmembrane helix orientation, J. Biol. Chem. 284 (2009) 6079–6092.
[36] M. Johnsson, N. Bergstrand, K. Edwards, J.J.R. Stålgren, Adsorption of a PEO − PPO − PEO triblock copolymer on small unilamellar vesicles: equilibrium and kinetic properties and correlation with membrane permeability, Langmuir 17 (2001) 3902–3911.
[37] E. Reimhult, F. Hook, B. Kasemo, Intact vesicle adsorption and supported biomembrane formation from vesicles in solution: influence of surface chemistry, vesicle size, temperature, and osmotic pressure, Langmuir 19 (2003) 1681–1691.
[38] M.V. Voinova, M. Rodahl, M. Jonson, B. Kasemo, Viscoelastic acoustic response of layered polymer films at fluid-solid interfaces: continuum mechanics approach, Phys. Scr. 59 (1999) 391–396.
[39] C.A. Keller, B. Kasemo, Surface specific kinetics of lipid vesicle adsorption measured with a quartz crystal microbalance, Biophys. J. 75 (1998) 1397–1402.
[40] J.M. Boggs, Lipid intermolecular hydrogen bonding: influence on structural organization and membrane function, Biochim. Biophys. Acta Rev. Biomembr. 906 (1987) 353–404.
[41] J. Hoyo, E. Guaus, J. Torrent-Burgues, F. Sanz, Electrochemical behaviour of mixed LB films of ubiquinone - DPPC, J. Electroanal. Chem. 669 (2012) 6–13.
[42] Y.F. Chen, K.Y. Tsang, W.F. Chang, Z.A. Fan, Differential dependencies on [Ca2+] and temperature of the monolayer spontaneous curvatures of DOPE, DOPA and cardiolipin: effects of modulating the strength of the inter-headgroup repulsion, Soft Matter 11 (2015) 4041–4053.
[43] D. Kashchiev, D. Exerowa, Bilayer lipid membrane permeation and rupture due to hole formation, Biochim. Biophys. Acta Biomembr. 732 (1983) 133–145.
[44] S. Paula, A.G. Volkov, A.N. VanHoek, T.H. Haines, D.W. Deamer, Permeation of protons, potassium ions, and small polar molecules through phospholipid bilayers as a function of membrane thickness, Biophys. J. 70 (1996) 339–348.
[45] G. Olofsson, E. Sparr, Ionization constants pKa of cardiolipin, PLoS One 8 (2013) e73040.
[46] R.N.A.H. Lewis, D.A. Mannock, R.N. McElhaney, Chapter 2 membrane lipid molecular structure and polymorphism, in: M.E. Richard (Ed.), Current Topics in Membranes, Academic Press, 1997, pp. 25–102.
[47] R.N.A.H. Lewis, R.N. McElhaney, Surface charge markedly attenuates the nonlamellar phase-forming propensities of lipid bilayer membranes: calorimetric and 31P-nuclear magnetic resonance studies of mixtures of cationic, anionic, and zwitterionic lipids, Biophys. J. 79 (2000) 1455–1464.
[48] G.L. Powell, D. Marsh, Polymorphic phase-behavior of cardiolipin derivatives studied by P-31 NMR and X-ray-difraction, Biochemistry 24 (1985) 2902–2908.
[49] J.M. Seddon, R.D. Kaye, D. Marsh, Induction of the lamellar-inverted hexagonal phase transition in cardiolipin by protons and monovalent cations, Biochim. Biophys. Acta Biomembr. 734 (1983) 347–352.
[50] R.P. Rand, S. Sengupta, Cardiolipin forms hexagonal structures with divalent cations, Biochim. Biophys. Acta Biomembr. 255 (1972) 484–492.
[51] R.N.A.H. Lewis, R.N. McElhaney, The physicochemical properties of cardiolipin bilayers and cardiolipin-containing lipid membranes, Biochim. Biophys. Acta Biomembr. 1788 (2009) 2069–2079.
[52] J.D. Unsay, K. Cosentino, Y. Subburaj, A.J. García-Sáez, Cardiolipin effects on membrane structure and dynamics, Langmuir 29 (2013) 15878–15887.
[53] B. Kollmitzer, P. Heftberger, M. Rappolt, G. Pabst, Monolayer spontaneous curvature of raft-forming membrane lipids, Soft Matter 9 (2013) 10877–10884.
[54] S.J. Slater, C. Ho, F.J. Taddeo, M.B. Kelly, C.D. Stubbs, Contribution of hydrogen bonding to lipid-lipid interactions in membranes and the role of lipid order: effects of cholesterol, increased phospholipid unsaturation, and ethanol, Biochemistry 32 (1993) 3714–3721.
[55] P. Wessman, A.A. Stromstedt, M. Malmsten, K. Edwards, Melittin-lipid bilayer interactions and the role of cholesterol, Biophys. J. 95 (2008) 4324–4336.
[56] R.M. Epand, R. Bottega, Modulation of the phase transition behavior of phosphatidylethanolamine by cholesterol and oxysterols, Biochemistry 26 (1987) 1820–1825.
[57] B. Perly, I.C. Smith, H.C. Jarrell, Effects of replacement of a double bond by a cyclopropane ring in phosphatidylethanolamines: a 2H NMR study of phase transitions and molecular organization, Biochemistry 24 (1985) 1055–1063.
[58] J.C. Gomez-Fernandez, M.A. Llamas, F.J. Aranda, The interaction of coenzyme Q with phosphatidylethanolamine membranes, Eur. J. Biochem. 259 (1999) 739–746.
[59] K. Matsuzaki, K. Sugishita, N. Ishibe, M. Ueha, S. Nakata, K. Miyajima, R.M. Epand, Relationship of membrane curvature to the formation of pores by magainin 2, Biochemistry 37 (1998) 11856–11863.
[60] V.V. Malev, L.V. Schagina, P.A. Gurnev, J.Y. Takemoto, E.M. Nestorovich, S.M. Bezrukov, Syringomycin E channel: a lipidic pore stabilized by lipopeptide? Biophys. J. 82 (2002) 1985–1994.
[61] A.A. Sobko, E.A. Kotova, Y.N. Antonenko, S.D. Zakharov, W.A. Cramer, Effect of lipids with different spontaneous curvature on the channel activity of colicin E1: evidence in favor of a toroidal pore, FEBS Lett. 576 (2004) 205–210.
[62] G. Daum, J.E. Vance, Import of lipids into mitochondria, Prog. Lipid Res. 36 (1997) 103–130.
[63] J. Malcolm East, Membrane Structural Biology With Biochemical and Biophysical Foundations, Taylor & Francis, 2008.
[64] A.G. Lee, Lipids and their effects on membrane proteins: evidence against a role for fluidity, Prog. Lipid Res. 30 (1991) 323–348.
[65] A.N. Dickey, R. Faller, Behavioral differences between phosphatidic acid and phosphatidylcholine in the presence of the nicotinic acetylcholine receptor, Biophys. J. 95 (2008) 5637–5647.
[66] G. Paradies, V. Paradies, V. De Benedictis, F.M. Ruggiero, G. Petrosillo, Functional role of cardiolipin in mitochondrial bioenergetics, Biochim. Biophys. Acta Bioenerg. 1837 (2014) 408–417.
[67] M. Ren, C.K.L. Phoon, M. Schlame, Metabolism and function of mitochondrial cardiolipin, Prog. Lipid Res. 55 (2014) 1–16.
[68] J.B. Massey, Interfacial properties of phosphatidylcholine bilayers containing vitamin E derivatives, Chem. Phys. Lipids 109 (2001) 157–174.
[69] C. Wollstein, M. Winterhalter, S.S. Funari, The location of coenzyme Q10 in phospholipid membranes made of POPE: a small-angle synchrotron X-ray diffraction study, Eur. Biophys. J. Biophys. Lett. 44 (2015) 373–381.
[70] A. Ausili, A. Torrecillas, F. Aranda, A.D. Godos, S. Sánchez-Bautista, S. Corbalán-García, J.C. Gómez-Fernández, Redox state of coenzyme Q10 determines its membrane localization, J. Phys. Chem. B 112 (2008) 12696–12702.